Physics Letters B 733 (2014) 89–92

Contents lists available at ScienceDirect

Physics Letters B

www.elsevier.com/locate/physletb

Insights into low-energy elastic scattering of halo nuclei

Alexis Diaz-Torres [a,*], Antonio M. Moro [b]

[a] ECT, Villa Tambosi, I-38123 Villazzano, Trento, Italy
[b] Departmento de FAMN, Universidad de Sevilla, Sevilla, Spain

ARTICLE INFO

Article history:
Received 18 January 2014
Received in revised form 14 April 2014
Accepted 14 April 2014
Available online 18 April 2014
Editor: J.-P. Blaizot

Keywords:
Elastic scattering
Coulomb-nuclear interference
Halo nuclei
Open quantum systems

ABSTRACT

Recent measurements of low-energy (quasi)elastic-scattering angular distribution of halo nuclei have shown a strong suppression of the Coulomb-nuclear interference peak. Examining the components of the elastic-scattering differential cross sections for ^{11}Be + ^{64}Zn and ^{6}He + ^{208}Pb at energies near the Coulomb barrier, this appears to be caused by a dramatic phase-change (destructive) of the reduced Coulomb-nuclear interference term due to continuum couplings.

Quantum coherence among probability amplitudes is a remarkable aspect in nature, which results in quantum interference effects. It can be observed in interferometry of matter-waves ranging from electrons to complex molecules like C_{70}-fullerenes [1]. The visibility of the interference fringes can be reduced by coherence loss due to the interaction between the matter-waves and an environment composed of gas particles [1], laser photons [2] or the electron and phonon gas inside a semiconductor plate [3]. The dynamics of an open quantum system [4] may also be revealed in the elastic scattering of halo nuclei [5] – a conventional core nucleus surrounded by a loosely bound halo of orbiting neutron(s) or proton(s), as the elastic channel (sub-system) strongly interacts with the continuum of breakup channels (environment). This interaction entangles the two systems and may distribute coherence over so many states as to render it negligible in the subsystem [6].

Elastic scattering of ^{6}He and ^{11}Li by a ^{208}Pb target at energies near the Coulomb barrier shows a strong reduction of the Coulomb-nuclear (CN) interference peak [7–9]. The same happens in the quasielastic scattering of ^{11}Be by a ^{64}Zn target, when this peak is compared to the one in the elastic scattering of the ^{9,10}Be stable projectiles [10,11]. The latter has been interpreted within the optical model (OM) and the continuum-discretized coupled-channels (CDCC) framework [10,11]. The OM analysis [10] suggests a long-range absorption that is not provided by a simple, dipole-Coulomb dynamical polarization potential [11]. This is indicative that long-range nuclear couplings are critical, as demonstrated by the CDCC analysis which explains the observations fairly well (Fig. 1). In Fig. 1, the CDCC and OM curves (solid and long dashed lines, respectively) are shown along with the one-channel calculation (short dashed line) which resembles the CN interference peak for the stable isotopes. Elastic heavy-ion scattering at small angles has also been interpreted as a Coulomb rainbow or Fresnel diffraction phenomenon [14], which seems to be inadequate and better characterized as a phenomenon of CN interference [15].

This paper provides insights into the elastic-scattering angular distribution of both ^{11}Be + ^{64}Zn at $E_{c.m.} \approx 24.5$ MeV [10,11] and ^{6}He + ^{208}Pb at $E_{c.m.} \approx 26.2$ MeV [7], addressing their different components. The established formula of the elastic differential cross section in scattering by Coulomb and nuclear potentials [14], $d\sigma/d\Omega = |f_C(\theta) + f_N(\theta)|^2$, includes three terms: Coulomb, nuclear and their interference. It appears logical to associate the CN interference effects with the presence or absence of the CN interference peak [15]. The elastic differential cross section is usually normalized relative to the point-Coulomb (or Rutherford) scattering formula, as presented in Fig. 1:

$$\sigma/\sigma_R = 1 + \frac{|f_N(\theta)|^2}{|f_C(\theta)|^2} + \frac{2\,Re[f_C^*(\theta) f_N(\theta)]}{|f_C(\theta)|^2}. \quad (1)$$

The second and the third parts in Eq. (1) are the nuclear and the CN interference terms, respectively. Explicit expressions of the Coulomb and nuclear scattering amplitudes can be found in Chapter 4 of Ref. [14]. For simplicity, we call $f_N(\theta)$ the nuclear scattering amplitude, but this is a *Coulomb-modified* nuclear amplitude as it also includes both Coulomb phase shifts and

* Corresponding author.
E-mail address: torres@ectstar.eu (A. Diaz-Torres).

http://dx.doi.org/10.1016/j.physletb.2014.04.032

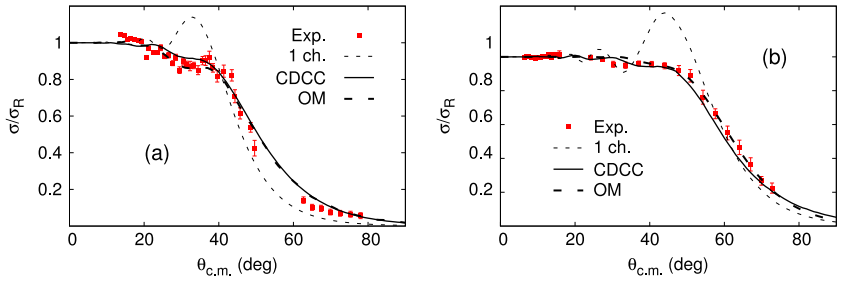

Fig. 1. (a) Measurements of quasielastic-scattering angular distribution for ^{11}Be + ^{64}Zn at $E_{c.m.} \approx 24.5$ MeV are compared to a number of model calculations [10,11]. The CN interference peak in the one-channel calculation is similar to the one for the ^{9,10}Be isotopes [10,11], which is suppressed for ^{11}Be. (b) The same for ^{6}He + ^{208}Pb at $E_{c.m.} \approx 26.2$ MeV [7,8,12]. The energies are ∼ 1.5–1.4 times the Sao Paulo potential barriers [13], respectively.

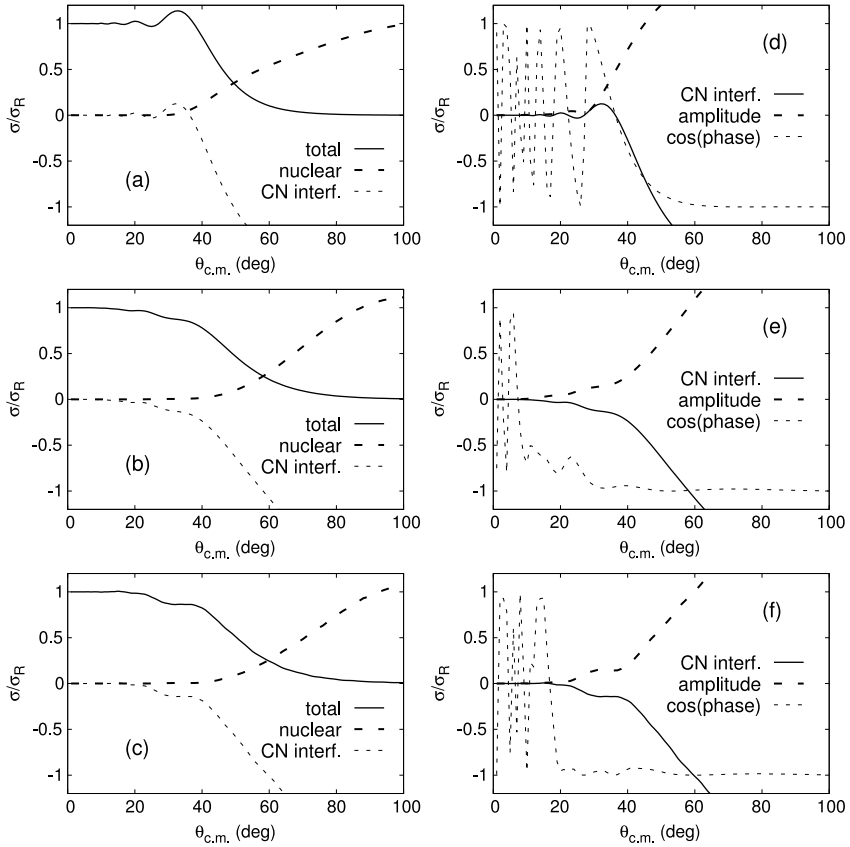

Fig. 2. (Left) Decomposition of the total elastic-scattering angular distribution for ^{11}Be + ^{64}Zn at $E_{c.m.} \approx 24.5$ MeV, within various model calculations: (a) one-channel, (b) converged full CDCC, and (c) the OM. The nuclear term changes almost in the same manner, whereas the CN interference term is different and dominant, determining the key features of the total distribution. (Right) Decomposition of the CN interference term into the product of its amplitude and cosine of its phase for (d) one-channel, (e) converged full CDCC, and (f) the OM calculations. The continuum couplings dramatically change the phase [comparing (d) to (e)], which differs from the OM at very forward angles [comparing (e) to (f)].

higher-order Coulomb coupling effects on the elastic partial-wave S-matrix elements, S_L [14]. The CN interference term can be written as $2|f_N(\theta)|/|f_C(\theta)|\cos(\phi_N - \phi_C)$, where $\phi_N - \phi_C$ is the phase of $f_C^*(\theta) f_N(\theta)$. Clearly, only the CN interference term in Eq. (1) can make $\sigma/\sigma_R < 1$, as the nuclear term is non-negative. The present work demonstrates that the CN interference term declines and becomes destructive in the angular region of the CN interference peak due to continuum couplings. These couplings produce a dynamic polarization potential with a long-range imaginary part [16], similar to the one in the elastic scattering of deformed heavy ions [17]. The breakup process yields a radially extended absorption which damps the S_L amplitude for partial waves beyond the grazing one, making $f_N(\theta) \approx -f_C(\theta) - \frac{1}{2ik}\sum_L (2L+1) P_L(\cos\theta)$, if $|S_L| \ll 1$ [18]. In that case, since the Legendre polynomials, $P_L(\cos\theta)$, are highly oscillating, the second term can be very small due to cancellation of terms with opposite signs, and equivalently $f_C(\theta)$ and $f_N(\theta)$ annihilate each other. At very forward angles, $f_N(\theta)$ is very small as $|S_L| \sim 1$, but weak oscillations in the differential cross section happen due to the CN interference effects (Fig. 1).

The nuclear and the CN interference terms in Eq. (1) are quantified as follows. Both collisions, ^{11}Be + ^{64}Zn and ^{6}He + ^{208}Pb, are treated within a three-body reaction model, namely, ^{10}Be + n + ^{64}Zn and ^{4}He + 2n + ^{208}Pb. Elastic S_L elements derived from (i) one-channel ($1/2^+$ and 0^+ ground-states of ^{11}Be and ^{6}He, respectively), (ii) the converged full CDCC, and (iii) the OM calculations are analyzed. These calculations are reported in Refs. [8,11,12], to which we refer for further details, and shown in Fig. 1. The CDCC outcomes are compared to the OM results, allowing us to evaluate

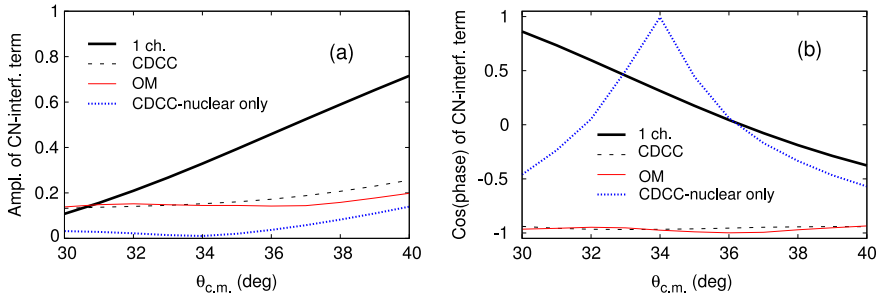

Fig. 3. (a) Amplitude and (b) cosine of the phase of the CN interference term for ^{11}Be + ^{64}Zn at $E_{c.m.} \approx 24.5$ MeV, in the angular region of the CN interference peak, with a number of model calculations. The product of (a) and (b) is the CN interference term. The coupling to the continuum strongly reduces the amplitude and changes the phase very much (comparing the thick solid to the short dashed line), which is described rather well by the OM (thin solid line). The combined effect of Coulomb and nuclear breakup couplings is crucial (comparing the short dashed to the dotted line).

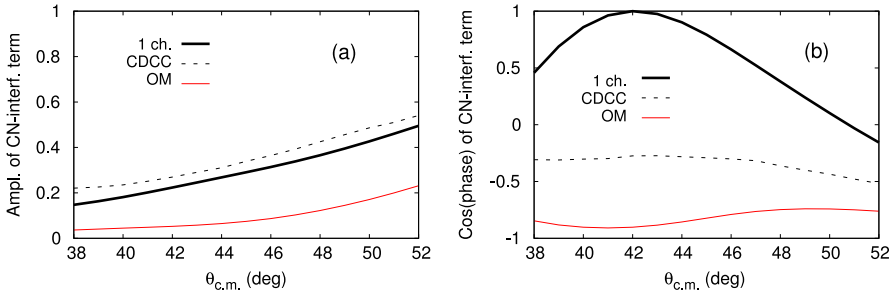

Fig. 4. The same as in Fig. 3 for ^{6}He + ^{208}Pb at $E_{c.m.} \approx 26.2$ MeV, in the angular region of the CN interference peak. The continuum couplings slightly increase the amplitude of the CN interference term, but its phase varies strongly (comparing the thick solid to the short dashed line). In contrast to Fig. 3, the CDCC and OM results disagree quantitatively.

to what extent the second and third terms in Eq. (1) are consistently given by both approaches. For ^{11}Be + ^{64}Zn, the fusion of both ^{10}Be and the valence neutron as well as the ^{10}Be and ^{64}Zn inelastic excitations are effectively included through optical potentials [11]. For ^{6}He + ^{208}Pb, an improved version of the two-body $\alpha + 2n$ model of ^{6}He is employed [12]. The $2n - ^{208}$Pb interaction is obtained by folding the $n - ^{208}$Pb optical potential with the $2n$-density from a three-body model of ^{6}He [12]. Results for ^{11}Be + ^{64}Zn are discussed first, followed by ^{6}He + ^{208}Pb.

The ^{11}Be + ^{64}Zn case. Fig. 2 (left) shows the decomposition of the total elastic-scattering angular distribution (solid line) into the nuclear (long dashed line) and the CN interference terms (short dashed line). It is observed that the nuclear term is nearly the same in all the calculations, whilst the CN interference is different, dominant and mainly destructive, determining the shape of the total elastic angular distribution. The CDCC results [panel (b)] are very similar to the phenomenological OM calculations [panel (c)]. In Fig. 2 (right), the CN interference term (solid line) is presented along with its amplitude (long dashed line) and cosine of its phase (short dashed line). Clearly, the continuum couplings dramatically change the phase [comparing the panel (d) to the panel (e)], which is not resembled by the phenomenological OM at very forward angles [panel (f)]. At these angles, high partial waves dominate; the amplitude of the interference term is nearly zero, as $f_N(\theta)$ is very small, while its rapidly oscillating phase is $\sim \ln[\sin^2(\theta/2)]$ deriving from $f_C^*(\theta)$ [14]. The angular region of the CN interference peak (30°–40°) is highlighted in Fig. 3, where it can be seen that the CN interference term very much declines in amplitude [panel (a)] and its phase changes dramatically [panel (b)] due to continuum couplings (comparing the thick solid to the short dashed line). The dotted line corresponds to a CDCC calculation including nuclear breakup only [11]. Comparing the dotted to the short dashed line, it appears that the combined effect of Coulomb and nuclear breakup couplings is essential for the features of the CN interference term. In this angular region, the CN interference term is two orders of magnitude larger than the nuclear term (not shown).

The ^{6}He + ^{208}Pb case. The decomposition of the total elastic differential cross section into the nuclear and the CN interference terms has the same features as in Fig. 2 (not shown). In Fig. 4, the angular region of the CN interference peak (38°–52°) is presented. Unlike the ^{11}Be + ^{64}Zn case, the continuum couplings slightly increase the amplitude of the CN interference term [panel (a)], but strongly decrease the cosine of its (destructive) phase [panel (b)]. Their product is the CN interference term that also declines. It also happens within the OM analysis [8] (thin solid line), although the OM and CDCC outcomes disagree quantitatively, unlike the ^{11}Be + ^{64}Zn case in Fig. 3.

In summary, within a realistic reaction model for ^{11}Be + ^{64}Zn and ^{6}He + ^{208}Pb at near-barrier energies, a detailed study of the terms of the elastic-scattering angular distribution demonstrates that the interference between the point-Coulomb and the Coulomb-modified nuclear scattering amplitudes – termed the Coulomb-nuclear interference – is crucial. The combined effect of Coulomb and nuclear interactions between the elastic channel and the high-density environment of breakup states leads to a dramatic phase-change of the Coulomb-nuclear interference term, making the interference effects destructive. The Coulomb-nuclear interference term is also reduced in magnitude. These features of the Coulomb-nuclear interference and the long-range absorption (loss of flux) are interconnected, and all of them are caused by the coupling to the continuum states. The destructive (and reduced) Coulomb-nuclear interference term suppresses the Coulomb-nuclear interference peak in the (quasi)elastic-scattering angular distribution, resembling the elastic scattering of deformed stable nuclei where the environment is small [19]. The continuum states provide a *large* environment, and the access to it from the sub-system (elastic channel) can be controlled by modifying key variables, such as (i) the incident energy, (ii) the breakup threshold of the halo projectile, and (iii) the strength of the (Coulomb

and nuclear) breakup couplings determined by the target nucleus. From the viewpoint of classical statistical mechanics, considering the large volume of the phase-space of the breakup fragments, the breakup process should be irreversible [20]. The *irreversible* dynamics of open quantum systems could be investigated through the low-energy elastic scattering of halo nuclei in the nuclear physics context [21–24].

Acknowledgements

A.D.-T. thanks Wolfram Weise for a careful reading of the paper and constructive suggestions and Ian Thompson and Jeff Tostevin for useful comments. A.M.M. is funded by the Spanish Ministerio de Ciencia e Innovación under project FPA2009-07653, and by the Spanish Consolider-Ingenio 2010 Programme CPAN (CSD2007-00042)

References

[1] K. Hornberger, et al., Phys. Rev. Lett. 90 (2003) 160401.
[2] D.A. Kokorowski, et al., Phys. Rev. Lett. 86 (2001) 2191.
[3] P. Sonnentag, F. Hasselbach, Phys. Rev. Lett. 98 (2007) 200402.
[4] H.-P. Breuer, F. Petruccione, The Theory of Open Quantum Systems, Oxford University Press, Oxford, 2002.
[5] A.S. Jansen, et al., Rev. Mod. Phys. 76 (2004) 215.
[6] L. Hackermüller, et al., Nature 427 (2004) 711.
[7] O.R. Kakuee, et al., Nucl. Phys. A 728 (2003) 339.
[8] A.M. Sánchez-Benítez, et al., Nucl. Phys. A 803 (2008) 30.
[9] M. Cubero, et al., Phys. Rev. Lett. 109 (2012) 262701.
[10] A. Di Pietro, et al., Phys. Rev. Lett. 105 (2010) 022701.
[11] A. Di Pietro, et al., Phys. Rev. C 85 (2012) 054607.
[12] A.M. Moro, et al., Phys. Rev. C 75 (2007) 064607.
[13] L.C. Chamon, et al., Phys. Rev. C 66 (2002) 014610.
[14] G.R. Satchler, Direct Nuclear Reactions, Clarendon Press, Oxford, 1983, p. 119.
[15] S.H. Fricke, et al., Nucl. Phys. A 500 (1989) 399.
[16] L. Borowska, et al., Phys. Rev. C 79 (2009) 044605.
[17] W.G. Love, et al., Nucl. Phys. A 291 (1977) 183.
[18] The formal partial-wave expansion of the Coulomb scattering amplitude is used, which is Eq. (4.23) in Ref. [14].
[19] M. Castagnino, et al., Mod. Phys. Lett. A 25 (2010) 1431.
[20] I.J. Thompson, A. Diaz-Torres, Prog. Theor. Phys. Suppl. 154 (2004) 69.
[21] E. Piasecki, et al., Phys. Rev. C 80 (2009) 054613.
[22] D.J. Hinde, et al., Nucl. Phys. A 834 (2010) 117c.
[23] N. Michel, et al., J. Phys. G 37 (2010) 064042.
[24] A. Diaz-Torres, Phys. Rev. C 82 (2010) 054617.